ACS OMEGA

http://pubs.acs.org/journal/acsodf Article

A Novel Conjugate Mechanism for Enhancing the Adsorption Capacity of Amine-Functionalized Activated Rice Husk Ash for Simultaneous Removal of Organics and Anions in Wastewater: Experimental and Theoretical Explanations

Phuoc Toan Phan, Trung Thanh Nguyen,* Surapol Padungthon, Thuy Nguyen Thi, and Nguyen Nhat Huy*

Cite This: *ACS Omega* 2022, 7, 28866–28874 Read Online

ACCESS | Metrics & More | Article Recommendations | Supporting Information

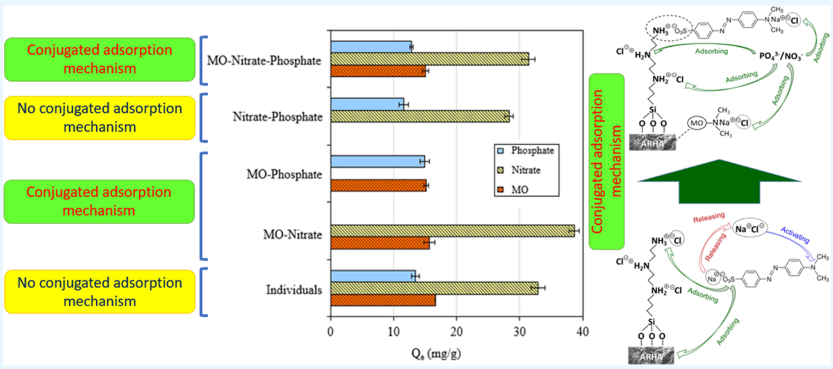

ABSTRACT: In this study, amine-functionalized rice husk ash (TRI-ARHA) was prepared and successfully applied as a multipurpose adsorbent for simultaneous removal of organics (i.e., methyl orange, MO), nitrate, and phosphate in wastewater with adsorption capacities of around 16.6 mgMO/g, 32.9 mgNO_3^--N/g, and 13.4 mgPO_4^{3-}-P/g. These capacities were superior to those of the other commercially available materials such as activated carbon and ion-exchange resins in both individual and multipollutant adsorption experiments. In addition, the simultaneous adsorption of three components gives a higher adsorption capacity than individual adsorption for each anion (e.g., 1.18 times for nitrate and 1.11 times for phosphate). A conjugated adsorption mechanism may occur on the surface of the TRI-ARHA material, which can be ascribed to the amine groups in the MO molecule that are further activated by H^+ (released from the surface amine groups) or Na^+ ions (present in the solution), to form new adsorption centers for nitrate and phosphate. The integration process of H^+ and Na^+ to the nitrogen positions of MO was also studied by computational chemistry with the basis set of B3LYP/6-32G* calculated by Gaussian 16 software. The application in the treatment of real wastewaters proved that the TRI-ARHA material was more advantageous for multipollutant removal than other materials, thanks to its conjugated adsorption mechanism.

1. INTRODUCTION

Wastewater contains many different pollutant components, which often include organic compounds and nutritional components such as nitrogen and phosphorus. For example, wastewater from livestock farming (e.g., swine and cow) is often treated by an anaerobic digester to recover biogas as fuel,[1] and after this decomposition process, the pollutant components in wastewater such as solids, organics, and nutrients (e.g., nitrogen and phosphorous) are still very high. The high contents of organics are the factors that seriously pollute surface water sources such as degradation of water quality due to oxygen deficiency and destruction of ecosystems in water bodies.[2] High nitrate levels can cause many health problems in humans such as blue baby syndrome (due to the formation of methemoglobin).[3] Meanwhile, phosphate is the main cause of water eutrophication.[4] Therefore, the development of a thorough and all-in-one technology for simultaneous treatment of these pollutants is necessary to effectively ensure the quality of the water before discharging into the water resources.

Received: March 30, 2022
Accepted: July 18, 2022
Published: August 9, 2022

For wastewater containing many pollutant components (e.g., organic matter, nitrogen, and phosphorus), the treatment process often has to combine many different works and treatment methods such as aerobic biological treatment, oxidation, precipitation, sedimentation, adsorption, or treatment by aquatic plants.[5] In particular, the adsorption units are usually designed as the last step when the pollutants are left in the wastewater at low concentrations that could not be removed by the previous stages.[6] In addition, wastewater from the textile dyeing process is polluted by various contaminants of colored organic compounds (e.g., organic compounds containing nitrogen) and nutrients (e.g., nitrate and phosphate). In addition, the adsorbers that are designed and constructed often have a relatively large volume due to the use of materials that can adsorb pollutants individually. Therefore, it is certain that developing a material capable of simultaneously adsorbing many pollutant components on different adsorption centers is essential and it is an effective solution to reduce the volume of the adsorber in the industry. Therefore, many studies focused on synthesizing a variety of multicomponent adsorbents,[7,8] especially for amine-grafted silica-based carriers.[9−12] These materials show very good adsorption capacity for both nitrate and phosphate in wastewater, thanks to the activity of amine groups, but they are almost not effective for adsorbing organic pollutants. In general, studies on synthesizing multipurpose adsorbents are also limited in both the number of studies and the number of adsorbates; thus, it is still a challenge and motivation for researchers in this research field.

Recently, rice husk ash has been considered as a potential source of raw material to fabricate a variety of multipurpose adsorbents.[13] Our group has used rice husk ash (RHA) from incinerators (e.g., brick kiln and agricultural drying combustion) as raw materials to produce an effective adsorbent for organic removal[14] and as a carrier for grafting amine groups to increase the adsorption activity for nitrate ions.[15,16] The results showed that RHA after surface activation with hydrofluoric acid (ARHA) has very good ability to adsorb organic matter, thanks to its porous structure and large specific surface area due to the partial dissolution of SiO_2, thus leaving the porous of high-carbon content.[14] Meanwhile, the amine-grafted on the ARHA carrier (TRI-ARHA) provides outstanding nitrate adsorption capacity, thanks to the strong activity of amine groups, the good bonds of Si in TRI and Si on ARHA, and the uniform dispersion of amines on the ARHA surface.[15,16] Thus, the TRI-ARHA material proves to be an effective material for many applications in environmental remediation as well as eliminating environmental pollution problems from waste RHA disposal. Therefore, the TRI-ARHA material promises to be a potential material in wastewater treatment applications, especially for wastewater containing multipollutants (e.g., organics and nutrients). However, there has not been any report on (i) the preparation and application of this material as a multipurpose adsorbent for effective and simultaneous removal of many pollutants and on (ii) the conjugate adsorption mechanism proposed from both experimental adsorption and computational chemistry.

In this study, TRI-ARHA was tested for the simultaneous adsorption of many components such as organics and nitrate and phosphate anions. This test aims to evaluate the ability and effectiveness of this material in the simultaneous removal of many pollution components. In addition, methyl orange was selected as an adsorbent with the goal of being a model organic compound with color and with an amine group to examine the adsorption enhancement for studying the insightful adsorption mechanism of the material.

2. MATERIALS AND METHODS

2.1. Chemicals. Methyl orange (powder form, denoted as MO), KNO_3, and KH_2PO_4 were used to prepare synthetic wastewater solutions containing MO, nitrate, and phosphate used in adsorption experiments. Hydrofluoric acid (HF) was used for activating RHA. 3-Aminopropyltriethoxysilane (APTES), *N*-[3-(trimethoxysilyl)-propyl]ethylenediamine (TMPED), *N*-[3-(trimethoxysilyl)-propyl]diethylenetriamine (TMPDT), toluene, and pentane were used in the process of grafting amines onto RHA. HCl was used to activate the material before adsorption. KBr was used in the Fourier transform infrared (FTIR) characterization of materials. Industrial-grade SiO_2 used was a commercial type and bought from a company in Ho Chi Minh City (Vietnam). Activated carbon (AC, Xilong, China) and commercial anion-exchange resin (Akualite A420, China) were used as reference adsorbents. Other chemicals such as H_2SO_4, NaOH, KCl, and deionized water were also used during the experiments. All chemicals are of analytical grade and bought from Merck, Sigma-Aldrich, or Xilong. The purity of chemicals in this study is the commonly used grades such as ACS (for MO, KNO_3, KH_2PO_4, and KBr), AR (for HF, toluene, pentane, HCl, H_2SO_4, NaOH, KCl, and SiO_2), and technical grade (for APTES, TMPED, and TMPDT).

2.2. Generation of Materials. To improve the porous structure, raw RHA was activated with HF followed a procedure in our previous study.[16] At first, 20 g of dry RHA was added into 800 mL of 5% HF solution at room temperature. After stirring time for 30 min, the solids were separated by filtration and washed several times with distilled water to neutral pH. The material was then dried overnight (12 h) at 110 °C to obtain the ARHA material. The A-SiO_2 material was synthesized with a similar process as ARHA using commercial SiO_2, as in our previous study.[17]

The incorporation of amine functional groups on the surface of ARHA or A-SiO_2 is performed by a facile grafting method reported in our previous studies.[16−18] At first, 1 g of ARHA was added to a double-necked glass flask containing 150 mL of toluene under stirring, which was then added with 0.3 mL of deionized water and stirred for 30 min. The flask was subsequently placed in a silicone oil bath, which was put on a magnetic stirrer and heater, and stabilized at a temperature of 85 °C. Next, 3 mL of triamine silane was added to the mixture and continuously stirred for 16 h. After this, the mixture was filtrated and washed with a similar amount of toluene and then pentane before being dried at 100 °C for 1 h to obtain the TRI-ARHA material. Before each adsorption experiment, the TRI-ARHA material was activated with 0.1 M HCl solution for 3 h at a ratio of 1 g/L, then separated using a filter, and left for drying overnight.

2.3. Material Characterizations. The specific surface area of the material was determined by N_2 adsorption−desorption isotherms at 77 K using a BET sorptometer (CBET 210A, PMI, USA). The crystalline structure of the materials was determined by X-ray diffraction (XRD) using a D2 Phaser diffractometer (XRD 300W, Bruker, Germany) equipped with Cu Kα radiation (λ = 1.5406 Å) at a step scan of 0.01° and a scan speed of 0.01°/30 s. The surface chemical composition of the material was determined by FTIR spectroscopy (Alpha,

https://doi.org/10.1021/acsomega.2c01955
ACS Omega 2022, 7, 28866−28874

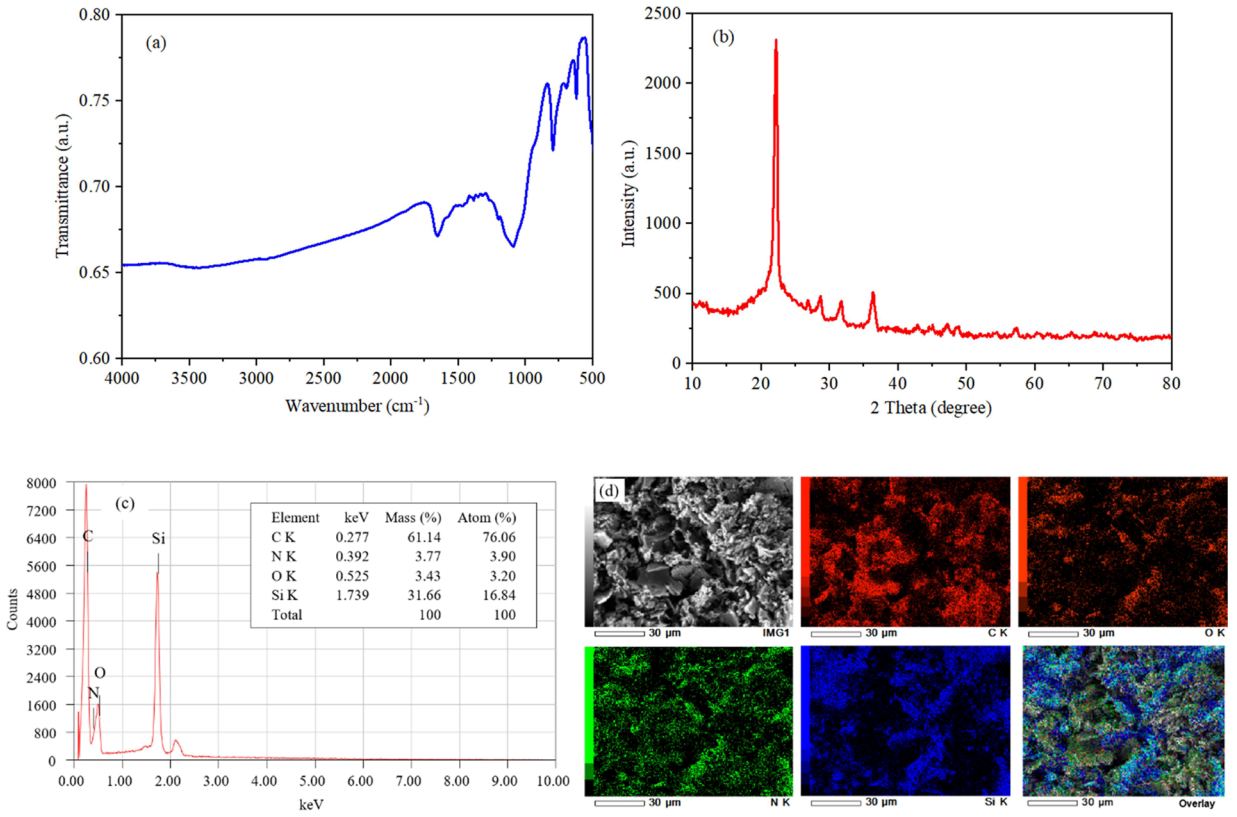

Figure 1. Results of (a) FTIR, (b) XRD, (c) EDX, and (d) SEM mapping of the TRI-ARHA material.

Bruker, Germany) with a conventional scanning spectrum from 500 to 4000 cm^{-1}.

2.4. Batch Adsorption Experiments. The removal of MO, nitrate, and phosphate was performed in batch experiments in the laboratory. In a typical test, 30 mg of adsorbent was added into a 100 mL conical flask containing 50 mL of synthetic wastewater (10 mgMO/L, 50 mgNO_3^--N/L, and 10 mgPO_4^{3-}-P/L). The mixture was stirred at 120 rpm at room temperature (~30 °C) and atmospheric pressure (~1 atm) for the adsorption process. After 30 min, the adsorbent was separated by centrifugation at 10,000 rpm for 10 min. The remaining MO concentration in the solution after adsorption was analyzed by UV−vis spectroscopy (SPECORD 210, Analytik Jena, Germany) at 464 nm. The nitrate concentration was determined according to TCVN 4562:1988 (Vietnam standard: Wastewater—Method of determining nitrate content), and the phosphate concentration was determined according to TCVN 6202:2008 (Vietnam standard: Water quality − Determination of phosphorus − Spectrometric method using ammonium molybdate). In the actual wastewater test, the chemical oxygen demand (COD) was determined according to TCVN 6491:1999 (Vietnam standard: Water quality—Determination of chemical oxygen demand). For total nitrogen (TN) and total phosphorous (TP) measurements, the sample was first digested by the persulfate method and then analyzed by the corresponding nitrate and phosphate analytical methods, respectively. Biochemical oxygen demand (BOD_5) was determined according to TCVN 6001-1:2008 (Vietnam standard: Water quality—Determination of biochemical oxygen demand). Each experiment was repeated at least three times, and the average value of adsorption capacity (Q_e, mg/g) of the material was calculated using eq 1.

$$Q_e = \frac{C_0 - C_e}{m} \times V \quad (1)$$

where C_0 and C_e (mg/L) are the initial and equilibrium concentrations of the pollutants in the solution, V (mL) is the volume of the solution, and m (mg) is the mass of the adsorbent.

2.5. Theoretical Calculation. Theoretical calculations were performed using Gaussian 16 software and were carried out on a Tohoku computer (Japan). To study the protonation of MO molecules in the aqueous environment, the calculation method uses the basis function set of B3LYP/6-31G* to optimize the structure and energy. In addition, the structures of the transition states are determined by minimizing the norm of the energy gradients.

3. RESULTS AND DISCUSSION

3.1. Characteristics of the TRI-ARHA Material. The TRI-ARHA material was synthesized following a process previously developed by our group[16] with material characteristics shown in Figure 1. From the FTIR result (Figure 1a), it is observed that the material has characteristic vibrations such as Si−H bonding (620−912 cm^{-1}), Si−O−Si (1091 cm^{-1}), C═C (1655 cm^{-1}), CH (2934 cm^{-1}), and −OH (3424 cm^{-1}) and stretching oscillation of the amine group was found at a wavenumber position of 1480 cm^{-1}.[16,19] From the XRD result (Figure 1b), the diffraction characteristic peaks for the cristobalite crystalline phase of silica in the RHA structure were clearly observed at 2θ of 22, 28.5, 31.5, and 36.3°. This result is consistent with previous studies on the RHA structure by Bhagiyalakshmi et al.[20] and Serra et al.[21] The energy-dispersive X-ray spectroscopy (EDX) and scanning electron microscopy (SEM) mapping results (Figure 1c,d) show that

https://doi.org/10.1021/acsomega.2c01955
ACS Omega 2022, 7, 28866−28874

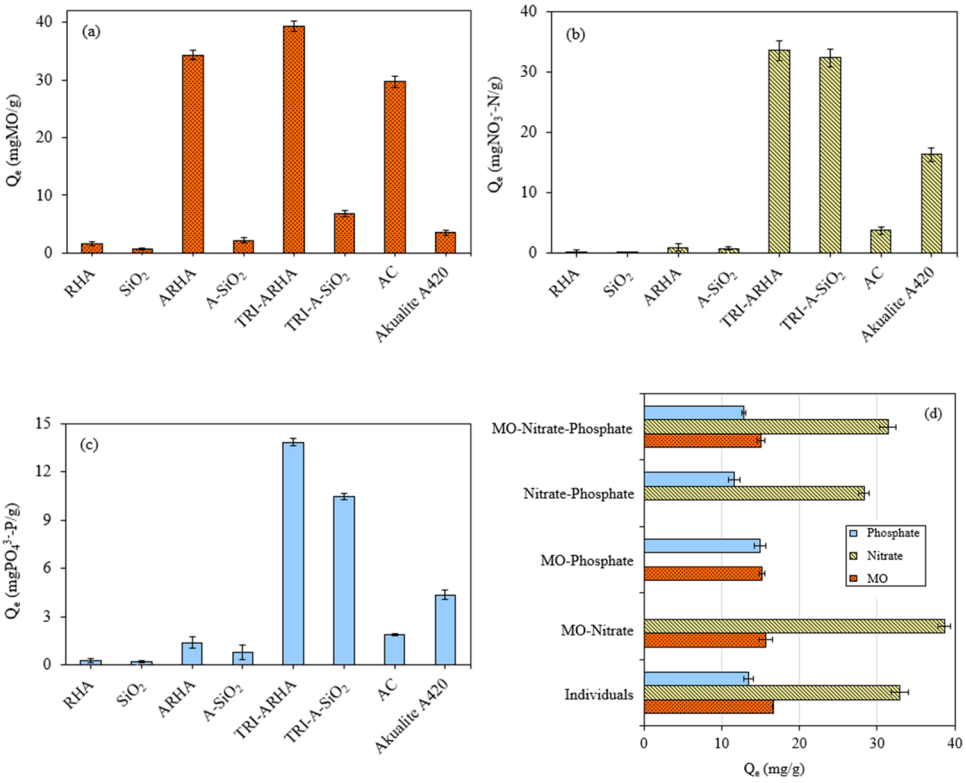

Figure 2. Adsorption capacity of different materials for (a) MO, (b) nitrate, and (c) phosphate and (d) individual and simultaneous adsorption of MO, nitrate, and phosphate.

the TRI-ARHA material contains elements of C, Si, O, and N with weight percentages of 61.14, 31.66, 3.43, and 3.77%, respectively, which are very well dispersed on the surface of the material. In addition, the pH at the zero point charge of the prepared TRI-ARHA was determined to be 5.9 (Figure S1 of the Supporting Information).

3.2. Multipurpose Adsorption Performance of TRI-ARHA. The adsorption performance of TRI-ARHA for both individual and simultaneous removal of MO, nitrate, and phosphate is demonstrated in Figure 2. In addition, the preliminary test results to investigate the effects of pH and TRI-ARHA dosage on MO, nitrate, and phosphate adsorption are shown in Figures S2 and S3. For MO adsorption (Figure 2a), the MO adsorption capacity of the TRI-ARHA material was compared with those of commercial materials (AC and Akualite A420) and other control materials (RHA, SiO_2, ARHA, A-SiO_2, and TRI-A-SiO_2). The high adsorption capacity for MO was observed for TRI-ARHA, ARHA, and AC, while the remaining control materials (RHA, SiO_2, A-SiO_2, TRI-A-SiO_2, and Akualite A420) have lower or negligible MO adsorption capacity. Specifically, the TRI-ARHA material has the highest MO adsorption capacity, which was 1.14 and 1.32 times higher than those of ARHA and AC, respectively. When replacing the ARHA carrier with A-SiO_2, the TRI-ARHA material has a higher MO adsorption capacity than TRI-A-SiO_2 by 5.78 times. The superior MO adsorption capacity of the TRI-ARHA material would be due to the outstanding characteristics of the ARHA carrier combined with the activity of the grafted triamine groups on the surface of the material. Comparing the MO adsorption capacity of ARHA and TRI-ARHA, it can be seen that MO is adsorbed mostly on the ARHA carrier and partly on the amine centers of the TRI-ARHA material.

In nitrate adsorption (Figure 2b), the TRI-ARHA material also had the highest nitrate adsorption capacity, which was 1.04, 2.06, 8.95, and 34.8 times higher than those of TRI-A-SiO_2, Akualite A420, AC, and ARHA, respectively. In addition, the other materials were almost incapable of removing nitrate. The high nitrate adsorption capacity of TRI-ARHA could be due to the good interaction of the amine groups with the ARHA composition and structure, thus resulting in a high-grafted amine content and its good dispersion on the surface of the TRI-ARHA material.[16] In phosphate adsorption (Figure 2c), raw materials (e.g., RHA and SiO_2) and carriers (e.g., ARHA and A-SiO_2) had very low or negligible phosphate adsorption efficiency. Meanwhile, the TRI-ARHA material had very good phosphate adsorption efficiency, which was 1.32, 3.18, 7.37, and 10 times higher than those of TRI-A-SiO_2, Akualite A420, AC, and ARHA, respectively. This result once again shows that the amine grafting on the ARHA carrier provides superior phosphate adsorption capacity for the TRI-ARHA material.

In the field of water and wastewater treatment, materials capable of simultaneous removal of organic components and nutrients such as nitrate and phosphate are difficult to find. As shown in Figure 2d, the TRI-ARHA material had the ability to simultaneously adsorb all three types of pollutants of organics, nitrate, and phosphate. In the case of individual adsorption, TRI-ARHA was able to remove ~16.6 mgMO/g, 32.9 $mgNO_3^-$-N/g, and 13.4 $mgPO_4^{3-}$-P/g, which slightly decreased to 15.1 mgMO/g, 31.4 $mgNO_3^-$-N/g, and 12.8 $mgPO_4^{3-}$-P/g. This reduction is due to the interaction and adsorption competition between the MO, nitrate, and phosphate components on the surface of the TRI-ARHA adsorbent. However, it is remarkable that the negative competition takes place only between the nitrate and

https://doi.org/10.1021/acsomega.2c01955
ACS Omega 2022, 7, 28866−28874

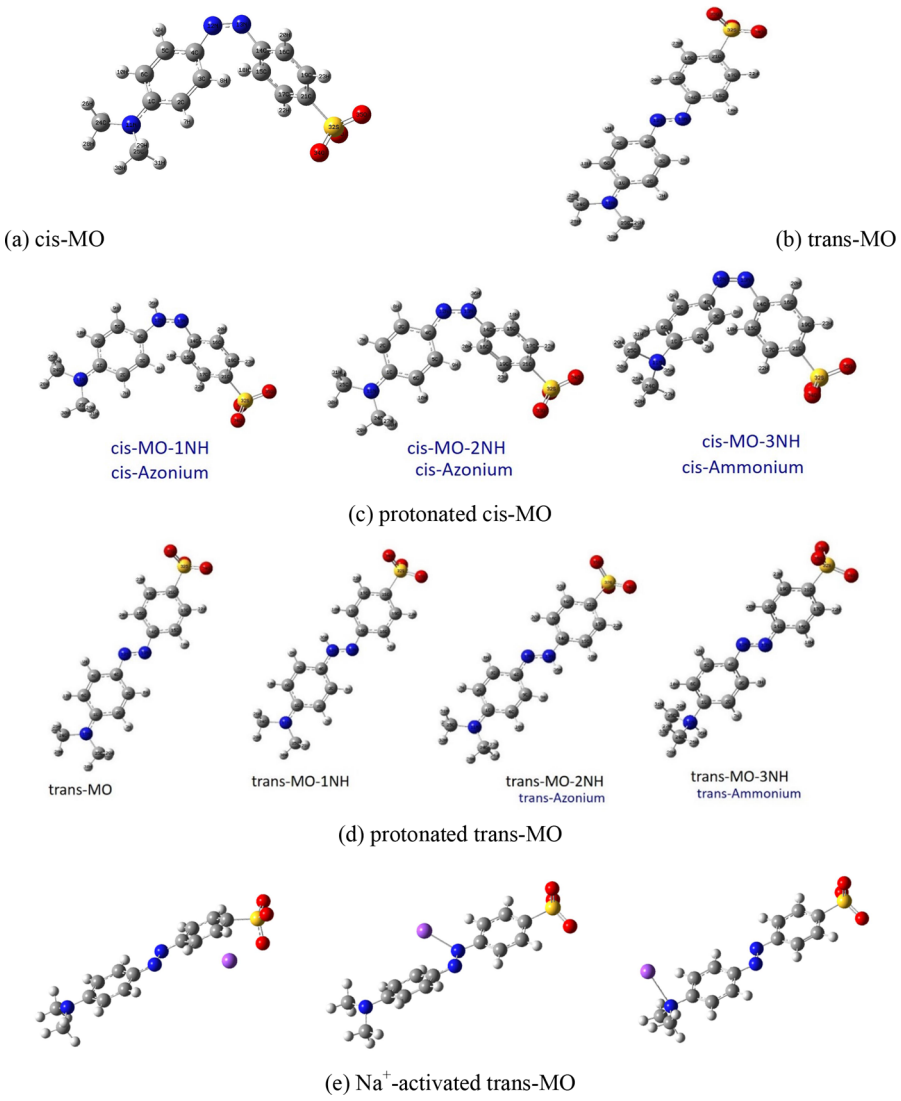

Figure 3. Optimal structures of MO: (a) *cis*-MO, (b) *trans*-MO, (c) protonated *cis*-MO, (d) protonated *trans*-MO, and (e) Na^+-activated *trans*-MO compounds.

phosphate components, while MO has a positive effect on the adsorption capacity for both nitrate and phosphate. Specific results in the adsorption experiment for two components MO−nitrate and MO−phosphate both illustrate a higher increase in nitrate and phosphate adsorption capacity (38.7 mgNO_3^--N/g and 14.9 mgPO_4^{3-}-P/g) than in the adsorption test without MO (28.3 mgNO_3^--N/g and 11.6 mgPO_4^{3-}-P/g). Therefore, the existence of MO has a positive effect on the adsorption of nitrate and phosphate, and it is possible that the amine or azo groups in MO act as supplementary active sites for the adsorption of nitrate, phosphate, or MO. However, in order to have a basis to propose this adsorption mechanism, it is necessary to study the process of activating the nitrogen center on the MO structure by protonation and Na^+ ion combination.

In addition, the BET specific surface area of the TRI-ARHA material before adsorption was 402 m^2/g. After adsorption of solutions containing nitrate and phosphate, the surface area reduced to 21.1 m^2/g. When simultaneously absorbing three components of nitrate, phosphate, and MO, the surface area further reduced to 2.44 m^2/g. These results further indirectly confirmed that anions such as nitrate and phosphate are adsorbed by the grafted amine groups on the surface of the material. Meanwhile, the adsorption of MO largely depends on the surface of ARHA. Therefore, when simultaneously absorbing three components of nitrate, phosphate, and MO, the active centers of the TRI-ARHA material for adsorption were employed almost completely.

3.3. Results from Theoretical Calculations. The structure of MO molecules with *cis*- and *trans*-isomers is shown in Figure 3a,b along with their energies shown in Table 1. The obtained results in Table 1 show that the energy levels of the *trans*-isomer of MO are lower than those of the *cis*-

Table 1. Computed Total Energy and Relative Energy Values of *cis*- and *trans*-Isomers of MO at the B3LYP/6-31G* Level of Theory

isomer	in vacuum		in water	
	E_{tot} (Hartree)	ΔE (kcal/mol)	E_{tot} (Hartree)	ΔE (kcal/mol)
trans-MO	−1330.000428	0.0	−1330.100884	0.0
cis-MO	−1329.977221	14.56	−1330.077937	14.40

https://doi.org/10.1021/acsomega.2c01955
ACS Omega 2022, 7, 28866−28874

Table 2. Computed Total Energy and Relative Energy Values of *cis*-MO and *trans*-MO Isomers and Their Protonated or Na^+-Activated Species at the B3LYP/6-31G* Level of Theory

in water	*cis*-MO	*cis*-MO-1NH	*cis*-MO-2NH	*cis*-MO-3NH
E_{tot} (Hartree)	−1330.077937	−1330.529173	−1330.538351	−1330.519619
ΔE (kcal/mol)		−283.15	**−288.91**	−277.16
in water	*trans*-MO	*trans*-MO-1NH	*trans*-MO-2NH	*trans*-MO-3NH
E_{tot} (Hartree)	−1330.100884	−1330.545843	−1330.553947	−1330.540826
ΔE (kcal/mol)		−279.22	**−284.30**	−276.07
in vacuum	*trans*-MO	*trans*-MO-1NNa	*trans*-MO-2NNa	*trans*-MO-3NNa
E_{tot} (Hartree)	−1330.000428	−1492.336791	−1492.304159	−1492.289305

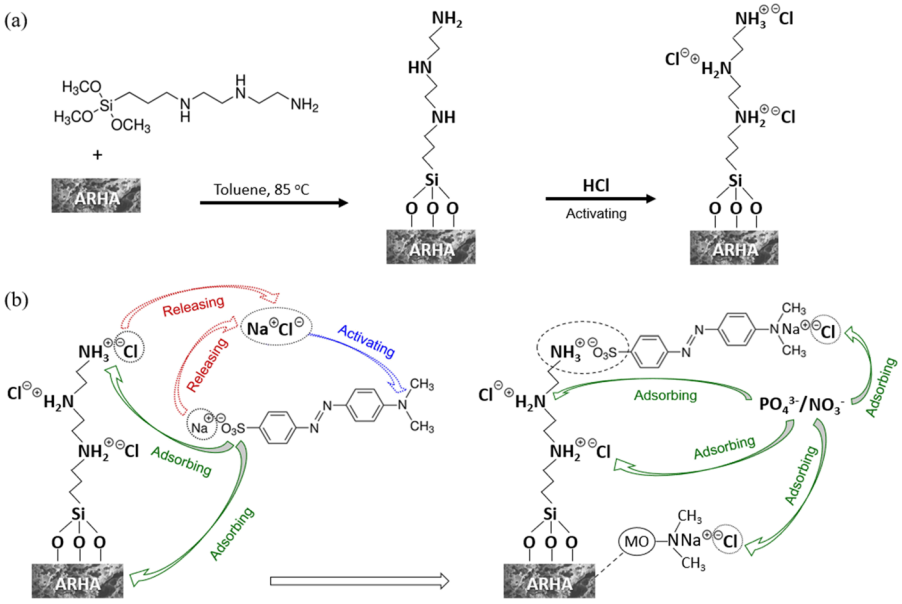

Figure 4. (a) Synthesis mechanism of TRI-ARHA and (b) its mechanism of the positive influence of MO on nitrate and phosphate adsorption.

isomer in both vacuum and water environments. Hence, it can be said that the *trans*-isomer structure of MO is more stable than the *cis*-isomer. The calculation results with Gaussian 16 software gave similar results as previously reported for the MO structure. In addition, this study focused on the adsorption process in an aqueous medium; therefore, subsequent computational studies were performed with the effect of aqueous solvents.

The protonation of MO is carried out as given in the following reaction:

$$MO + H_3O^+ \rightarrow MOH^+ + H_2O \quad (2)$$

Theoretical work on protonation was carried out by calculating the optimal structure and energy for protonation at the 1st, 2nd, and 3rd nitrogen positions of the *cis*-MO and *trans*-MO isomers. The protonation of the *cis*-isomer of MO was conducted in an aqueous medium with the optimal structure and energy shown in Figure 3c and Table 2 in which the protonated *cis*-MO structures at 1, 2, and 3 N positions were named *cis*-MO-1NH, *cis*-MO-2NH, and *cis*-MO-3NH, respectively. The results show that the protonation of MO at the second nitrogen position gives the smallest result, which also means that the protonation of MO prefers to produce *cis*-MO-2NH. Similar to that of *cis*-MO, the results from the protonation of the *trans*-MO isomer are displayed in Figure 3d and Table 2. In general, the protonation of MO for both *cis*- and *trans*-isomers takes place easily for the nitrogen at the 2nd position, which is in agreement with the calculation results of Azuki et al.[22] Similar to the protonation process, the activation of *trans*-MO by Na^+ ions was also performed but under a vacuum. As presented in Figure 3e and Table 2, the process of MO activation by Na^+ ions will be easily carried out at the first N position. In conclusion, the MO molecule is easily added by H^+ and Na^+ ions, where the conjugation of Na^+ ions to the MO structure is spontaneous and seems to be easier at the N position on the MO molecule compared to H^+ conjugation.

3.4. Mechanism for the Synthesis and Adsorption of TRI-ARHA. The positive influence of MO on the nitrate and phosphate adsorption capacities of the TRI-ARHA material is a very interesting finding. One hypothesis can be put forward to explain this phenomenon as the mechanism proposed in Figure 4. MO is an organic compound containing an amine group in its molecular structure; thus, it is adsorbed on the ARHA surface mainly by physical bonding via the ARHA porous carbon structure or partly by the amine centers of TRI-ARHA via an ion-exchange mechanism.[23,24] The adsorption of MO, nitrate, and phosphate by the ion-exchange mechanism on the amine centers of TRI-ARHA releases Cl^- ions into the solution, which then combine with Na^+ released from MO adsorption or H^+ present in solution to activate the amine group in the structure of MO.[25,26] This process is similar to the activation of the amine centers by HCl during the synthesis of the TRI-ARHA material (Figure 4a). Hence, this activation by Cl^- and Na^+ ions transforms the amine group in the MO structure into new adsorption sites that enhance the nitrate

https://doi.org/10.1021/acsomega.2c01955
ACS Omega 2022, 7, 28866−28874

and phosphate ion adsorption (Figure 4b). The utilization of Cl^- released from the amine centers after anion adsorption to activate other adsorption centers helps to avoid the change or contamination of the water source and is a novel role that cannot be found in the current anion-exchange resins. In addition, amine-grafted materials based on carriers of commercial SiO_2 or synthesized SiO_2 (e.g., MCM-41, MCM-48, and SBA-15) also do not have this function. This is considered the most outstanding advantage of RHA as a carrier for amine grafting to create an advanced TRI-ARHA material capable of simultaneously adsorbing three water contaminants of organics, nitrate, and phosphate. Therefore, it is of particular scientific significance to use RHA as the carrier in this study but not any other carriers.

The FTIR results of TRI-ARHA materials before and after adsorption in Figure 5 showed a change in the surface chemical

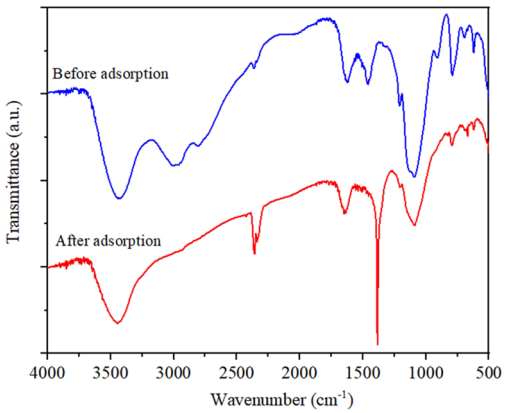

Figure 5. FTIR spectra of TRI-ARHA before and after adsorption of MO, nitrate, and phosphate.

composition of TRI-ARHA due to the adsorption of MO, nitrate, and phosphate. The TRI-ARHA material after adsorption still has the characteristic vibration peaks of the original material, but most of the characteristic peaks were observed at a lower intensity compared to the fresh TRI-ARHA sample, proving that there is an interaction of adsorbate molecules (MO, nitrate, and phosphate) on the surface of the TRI-ARHA material in which the overlapping stretching vibrations of $-OH$ and $-NH_2$ groups are determined by the presence of a peak at a position of 3424 cm^{-1}. The characteristic of the silica composition in the RHA structure is confirmed by Si−O−Si bonding at a peak of 1091 cm^{-1} and Si−H bonding at peaks from 620 to 912 cm^{-1}.[19] The peak at 1382 cm^{-1} represents the elongated N−O bond,[27] and its strong oscillation intensity demonstrates the efficient adsorption ability of TRI-ARHA. In addition, three clear peaks at 1625, 1458, and 1118 cm^{-1} in the spectrum of TRI-ARHA correspond to the elongated vibrations of C═O, C−N, and C−O, showing the presence of the protonated forms of triamine groups on the surface of the material.[3,27] After adsorption, the C−N peak (1458 cm^{-1}) shifted strongly to the elongated N−O peak (1382 cm^{-1}), indicating that ions such as nitrate were successfully attached to the adsorbent surface according to the mechanism of substitution of chloride ions at the amine groups as illustrated in the adsorption mechanism of Figure 6 and other studies.[26,28] Hence, the conjugated adsorption mechanism is the adsorption process that takes place at secondary adsorption sites. Here, the secondary adsorption sites are generated by the activation of functional groups of organic compounds that are adsorbed on the solid surface by suitable ions in solution.

3.5. Application of TRI-ARHA Materials in Actual Wastewater Treatment. In this experiment, actual wastewater samples were collected from a pond containing wastewater after a biogas digester from a household pig farm in the Cho Moi district (An Giang province, Vietnam). The collected wastewater sample was pretreated by filtering out suspended solids and then diluted to an appropriate concentration before being used for adsorption experiments. Results exhibited in Figure 7 showed that the TRI-ARHA material had good ability to simultaneously adsorb all three components of organic matter (COD of 42.5 mgO_2/g), nitrate (22.4 mgNO_3^--N/g), and phosphate (16.3 mgPO_4^{3-}-P/g). Meanwhile, AC only shows good organic adsorption capacity with a COD of 29.7 mgO_2/g but much less effective nitrate (3.15 mgNO_3^--N/g) and phosphate (2.32 mgPO_4^{3-}-P/g) adsorption. In contrast, the Akualite A420 resin well removes nitrate (10.6 mgNO_3^--N/g) and phosphate (9.87 mgPO_4^{3-}-P/g) but has poor adsorption for organic components (COD of 3.50 mgO_2/g). This result clearly shows the multicomponent adsorption advantage of the synthesized TRI-ARHA material compared to the two common commercial adsorbents of AC and the ion-exchange resin. This is very meaningful in the

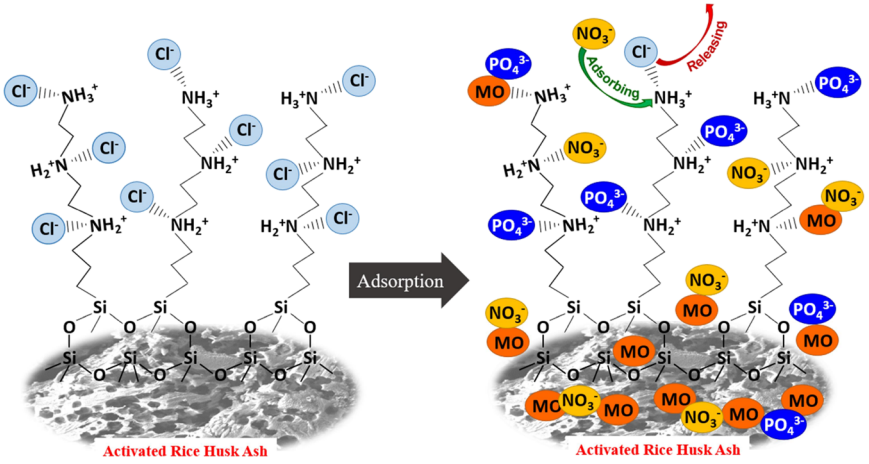

Figure 6. Proposed conjugate adsorption mechanism of the TRI-ARHA material.

https://doi.org/10.1021/acsomega.2c01955
ACS Omega 2022, 7, 28866−28874

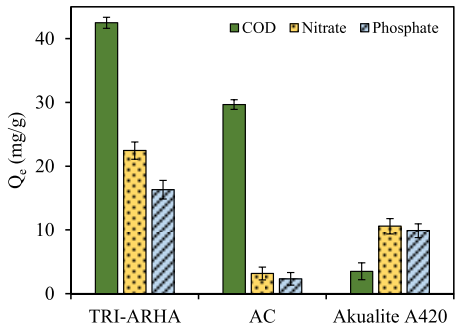

Figure 7. Simultaneous adsorption of organics, nitrate, and phosphate by the TRI-ARHA material compared with AC and a commercial ion-exchange resin in actual wastewater.

process of designing and constructing an adsorption tower in practice since it helps to reduce the volume of the adsorbent and limit the need to combine many different materials to achieve the treatment goal.

In order to specifically evaluate the actual wastewater treatment efficiency in comparison with the national technical regulations, the parameters BOD_5, TN, and TP of the initial and treated wastewater samples were measured. As depicted in Figure 8, the TRI-ARHA material gave a better treatment

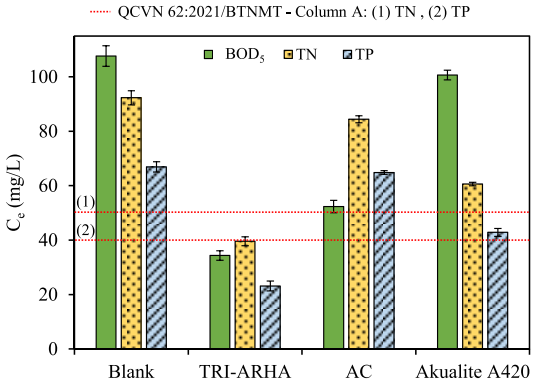

Figure 8. Concentrations of pollutants before and after being treated by TRI-ARHA, AC, and Akualite A420 compared to the discharge standard (QCVN 62:2021/BTNMT, Column A).

efficiency than AC and Akualite A420 resin in all three parameters of BOD_5, TN, and TP. Specifically, the actual wastewater sample had an initial concentration of 108 mgO_2/L for BOD_5, 92.3 mg/L for TN, and 66.9 mg/L for TP. After adsorption by the TRI-ARHA material, the remaining concentration was 34.3 mgO_2/L for BOD_5, 39.6 mg/L for TN, and 23.1 mg/L for TP, which were all lower than the maximum allowable values of the National Technical Regulation on Livestock Wastewater (QCVN 62:2021/BTNMT, Column A). Meanwhile, BOD_5, TN, and TP values after treatment were 52.3 mgO_2/L, 84.4 mg/L, and 64.8 mg/L, respectively, by using AC and 101 mgO_2/L, 60.6 mg/L, and 42.8 mg/L, respectively, by using Akualite A420, which do not meet the discharge standard (Figure 8).

4. CONCLUSIONS

This study successfully synthesized TRI-ARHA with a superior adsorption capacity for MO (16.6 mgMO/g), nitrate (32.9 $mgNO_3^-$-N/g), and phosphate (13.4 $mgPO_4^{3-}$-P/g) compared to reference materials (RHA, SiO_2, ARHA, A-SiO_2, and TRI-A-SiO_2) and commercial materials (AC and ion-exchange resin) in both individual and simultaneous adsorption tests. This is due to the outstanding characteristics of the ARHA carrier combined with the activity of the grafted triamine groups on the surface of the material and the conjugate adsorption proven by theoretical calculations and experiments of both synthetic and actual wastewaters.

■ ASSOCIATED CONTENT

Supporting Information

The Supporting Information is available free of charge at https://pubs.acs.org/doi/10.1021/acsomega.2c01955.

Determination of pH_{pzc} (point of zero charge) of the TRI-ARHA material (Figure S1); effect of pH of the adsorbate solution on its adsorption by TRI-ARHA (Figure S2); effect of the dosage of TRI-ARHA on the adsorption process (Figure S3); adsorption stability of TRI-ARHA after 10 regenerations (Figure S4); TG and DTG curves of the TRI-ARHA material (Figure S5); and SEM images of the TRI-ARHA material (a) before and (b) after adsorption (Figure S6) (PDF)

■ AUTHOR INFORMATION

Corresponding Authors

Trung Thanh Nguyen − *Laboratory of Nanomaterial, An Giang University, Long Xuyen City, An Giang Province 880000, Vietnam; Vietnam National University Ho Chi Minh City, Ho Chi Minh City 700000, Vietnam;* Phone: +84 907 101 590; Email: ntthanh@agu.edu.vn

Nguyen Nhat Huy − *Vietnam National University Ho Chi Minh City, Ho Chi Minh City 700000, Vietnam; Faculty of Environment and Natural Resources, Ho Chi Minh City University of Technology (HCMUT), Ho Chi Minh City 700000, Vietnam;* orcid.org/0000-0002-2918-7935; Phone: +84 901 964 985; Email: nnhuy@hcmut.edu.vn

Authors

Phuoc Toan Phan − *Laboratory of Nanomaterial, An Giang University, Long Xuyen City, An Giang Province 880000, Vietnam; Vietnam National University Ho Chi Minh City, Ho Chi Minh City 700000, Vietnam; Faculty of Environment and Natural Resources, Ho Chi Minh City University of Technology (HCMUT), Ho Chi Minh City 700000, Vietnam*

Surapol Padungthon − *Department of Environmental Engineering, Khon Kaen University, Khon Kaen 40002, Thailand*

Thuy Nguyen Thi − *Faculty of Environment and Natural Resources, Ho Chi Minh City University of Technology (HCMUT), Ho Chi Minh City 700000, Vietnam; Department of Environmental Engineering, International University, Ho Chi Minh City 700000, Vietnam*

Complete contact information is available at: https://pubs.acs.org/10.1021/acsomega.2c01955

Notes

The authors declare no competing financial interest.

■ ACKNOWLEDGMENTS

This research is funded by the Vietnam National University − Ho Chi Minh City under grant number A2020-16-01.

REFERENCES

(1) Aggarangsi, P.; Tippayawong, N.; Moran, J. C.; Rerkkriangkrai, P. Overview of livestock biogas technology development and implementation in Thailand. *Energy Sustain. Dev.* **2013**, *17*, 371−377.

(2) Chislock, M. F.; Doster, E.; Zitomer, R. A.; Wilson, A. E. Eutrophication: Causes, consequences, and controls in aquatic ecosystems. *Nat. Educ.* **2013**, *4*, 10−12.

(3) Aswin Kumar, I.; Viswanathan, N. Development and reuse of amine-grafted chitosan hybrid beads in the retention of nitrate and phosphate. *J. Chem. Eng. Data* **2018**, *63*, 147−158.

(4) Aswin Kumar, I.; Jeyaseelan, A.; Viswanathan, N.; Naushad, M.; Valente, A. J. M. Fabrication of lanthanum linked trimesic acid as porous metal organic frameworks for effective nitrate and phosphate adsorption. *J. Solid State Chem.* **2021**, *302*, No. 122446.

(5) Azizi, S.; Bayat, B.; Tayebati, H.; Hashemi, A.; Pajoum Shariati, F. Nitrate and phosphate removal from treated wastewater by Chlorella vulgaris under various light regimes within membrane flat plate photobioreactor. *Environ. Prog. Sustainable Energy* **2021**, *40*, No. e13519.

(6) Kumar, I. A.; Jeyaseelan, A.; Ansar, S.; Viswanathan, N. A facile synthesis of 2D iron bridged trimesic acid based MOFs for superior nitrate and phosphate retention. *J. Environ. Chem. Eng.* **2022**, *10*, No. 107233.

(7) Prashantha Kumar, T. K. M.; Mandlimath, T. R.; Sangeetha, P.; Revathi, S. K.; Ashok Kumar, S. K. Nanoscale materials as sorbents for nitrate and phosphate removal from water. *Environ. Chem. Lett.* **2018**, *16*, 389−400.

(8) Wiriyathamcharoen, S.; Sarkar, S.; Jiemvarangkul, P.; Nguyen, T. T.; Klysubun, W.; Padungthon, S. Synthesis optimization of hybrid anion exchanger containing triethylamine functional groups and hydrated Fe(III) oxide nanoparticles for simultaneous nitrate and phosphate removal. *Chem. Eng. J.* **2020**, *381*, No. 122671.

(9) Hamoudi, S.; Saad, R.; Belkacemi, K. Adsorptive removal of phosphate and nitrate anions from aqueous solutions using ammonium-functionalized mesoporous silica. *Ind. Eng. Chem. Res.* **2007**, *46*, 8806−8812.

(10) Saad, R.; Belkacemi, K.; Hamoudi, S. Adsorption of phosphate and nitrate anions on ammonium-functionalized MCM-48: Effects of experimental conditions. *J. Colloid Interface Sci.* **2007**, *311*, 375−381.

(11) Safia, H.; Abir, E. N.; Maissa, B.; Khaled, B. Adsorptive removal of nitrate and phosphate anions from aqueous solutions using functionalised SBA-15: Effects of the organic functional group. *Can. J. Chem. Eng.* **2012**, *90*, 34−40.

(12) Toan, P. P.; Thanh, N. T.; Huy, N. N.; Hang, L. N.; Thich, L. T. Characterization and adsorption capacity of Amine-SiO_2 material for nitrate and phosphate removal. *Vietnam J. Sci. Technol.* **2019**, *57*, 484−490.

(13) Ahmaruzzaman, M.; Gupta, V. K. Rice Husk and Its Ash as Low-Cost Adsorbents in Water and Wastewater Treatment. *Ind. Eng. Chem. Res.* **2011**, *50*, 13589−13613.

(14) Phuoc Toan, P.; Nguyen, T.-T.; Trang, N. Characterizations and methyl orange adsorption capacity of activated rice husk ash. *CTU J. Sci.* **2016**, *42*, 50−57.

(15) Phan, P. T.; Nguyen, T. A.; Nguyen, N. H.; Nguyen, T. T. Modelling approach to nitrate adsorption on triamine-bearing activated rice husk ash. *Eng. Appl. Sci. Res.* **2020**, *47*, 190−197.

(16) Phan, P. T.; Nguyen, T. T.; Nguyen, N. H.; Padungthon, S. Triamine-bearing activated rice husk ash as an advanced functional material for nitrate removal from aqueous solution. *Water Sci. Technol.* **2019**, *79*, 850−856.

(17) Phan, P. T.; Nguyen, T. T.; Nguyen, N. H.; Padungthon, S. A Simple Method for Synthesis of Triamine-SiO_2 Material toward Aqueous Nitrate Adsorption. *Environ. Nat. Resour. J.* **2019**, *17*, 59−67.

(18) Thanh, N. T. Amine-bearing activated rice husk ash for CO_2 and H_2S gas removals from biogas. *KKU Eng. J.* **2016**, *43*, 396−398.

(19) Ibrahim, D. M.; El-Hemaly, S. A.; Abdel-Kerim, F. M. Study of rice-husk ash silica by infrared spectroscopy. *Thermochim. Acta* **1980**, *37*, 307−314.

(20) Bhagiyalakshmi, M.; Yun, L. J.; Anuradha, R.; Jang, H. T. Synthesis of chloropropylamine grafted mesoporous MCM-41, MCM-48 and SBA-15 from rice husk ash: their application to CO_2 chemisorption. *J. Porous Mater.* **2010**, *17*, 475−484.

(21) Serra, M. F.; Conconi, S.; Gauna, M.; Suarez, G.; Aglietti, E. F.; Rendtorff, N. Mullite ($3Al_2O_3{\cdot}2SiO_2$) ceramics obtained by reaction sintering of rice husk ash and alumina, phase evolution, sintering and microstructure. *J. Asian Ceram. Soc.* **2016**, *4*, 61−67.

(22) Azuki, M.; Morihashi, K.; Watanabe, T.; Takahashi, O.; Kikuchi, O. Ab initio GB study of the acid-catalyzed cis−trans isomerization of methyl yellow and methyl orange in aqueous solution. *J. Mol. Struct.: THEOCHEM* **2001**, *542*, 255−262.

(23) Rehman, M. Z. U.; Aslam, Z.; Shawabkeh, R. A.; Hussein, I. A.; Mahmood, N. Concurrent adsorption of cationic and anionic dyes from environmental water on amine functionalized carbon. *Water Sci. Technol.* **2020**, *81*, 466−478.

(24) Lv, S.-W.; Liu, J.-M.; Ma, H.; Wang, Z.-H.; Li, C.-Y.; Zhao, N.; Wang, S. Simultaneous adsorption of methyl orange and methylene blue from aqueous solution using amino functionalized Zr-based MOFs. *Microporous Mesoporous Mater.* **2019**, *282*, 179−187.

(25) Smith, B. C. Organic nitrogen compounds V: Amine salts. *Spectroscopy* **2019**, *34*, 30−37.

(26) Song, W.; Gao, B.; Xu, X.; Wang, F.; Xue, N.; Sun, S.; Song, W.; Jia, R. Adsorption of nitrate from aqueous solution by magnetic amine-crosslinked biopolymer based corn stalk and its chemical regeneration property. *J. Hazard. Mater.* **2016**, *304*, 280−290.

(27) Rajeswari, A.; Amalraj, A.; Pius, A. Adsorption studies for the removal of nitrate using chitosan/PEG and chitosan/PVA polymer composites. *J. Water Process Eng.* **2016**, *9*, 123−134.

(28) Ebrahimi-Gatkash, M.; Younesi, H.; Shahbazi, A.; Heidari, A. Amino-functionalized mesoporous MCM-41 silica as an efficient adsorbent for water treatment: batch and fixed-bed column adsorption of the nitrate anion. *Appl. Water Sci.* **2017**, *7*, 1887−1901.

https://doi.org/10.1021/acsomega.2c01955
ACS Omega 2022, 7, 28866−28874